The Journal of Immunology

IDO Mediates TLR9-Driven Protection from Experimental Autoimmune Diabetes

Francesca Fallarino, Claudia Volpi, Teresa Zelante, Carmine Vacca, Mario Calvitti, Maria C. Fioretti, Paolo Puccetti, Luigina Romani and Ursula Grohmann

J Immunol 2009; 183:6303-6312; Prepublished online 19 October 2009;
doi: 10.4049/jimmunol.0901577
http://www.jimmunol.org/content/183/10/6303

The Journal of Immunology is published twice each month by
The American Association of Immunologists, Inc.,
1451 Rockville Pike, Suite 650, Rockville, MD 20852

Print ISSN: 0022-1767 Online ISSN: 1550-6606.

IDO Mediates TLR9-Driven Protection from Experimental Autoimmune Diabetes[1]

Francesca Fallarino,[2] Claudia Volpi,[2] Teresa Zelante, Carmine Vacca, Mario Calvitti, Maria C. Fioretti, Paolo Puccetti, Luigina Romani, and Ursula Grohmann[3]

Originally predicated on the recognition of an increasing prevalence of allergy, the hygiene hypothesis was later found to accommodate the contrasting epidemiologic trends in developed countries for infectious vs autoimmune diseases. Experimentally, reduced exposure to infections will increase the risk of disease in several models of experimental autoimmunity. Although TLRs were initially considered as stimulatory molecules capable of activating early defense mechanisms against invading pathogens, emerging data suggest that they can also exert a regulatory function. In the present study, we evaluated whether TLR3 and TLR9, recognizing microbial dsDNA and CpG-containing DNA sequences, respectively, play a role in the protection from experimental autoimmune diabetes induced in C57BL/6 mice by streptozotocin. In wild-type animals, the disease was accompanied by upregulation of IDO in pancreatic lymph nodes and would be greatly exacerbated by in vivo administration of an IDO inhibitor. Conversely, administration of a CpG-containing oligodeoxynucleotide greatly attenuated the disease in an IDO-dependent fashion. TLR9-, but not TLR3-deficient mice developed a more robust disease, an event accompanied by lack of IDO induction in pancreatic lymph nodes. Thus, our data suggest that the TLR9-IDO axis may represent a valuable target in the prevention/therapy of type 1 diabetes. *The Journal of Immunology,* **2009, 183: 6303–6312.**

Unlike the majority of organs and tissues in the human body, the immune system requires systematic environmental pressure to develop properly. Animals raised in a germfree environment acquire poorly efficient immunoregulatory mechanisms and are at a greater risk of diseases associated with immune dysfunction (1). The incidence of major infectious diseases has significantly decreased in developed countries over the last three decades. In parallel, the incidence of most autoimmune diseases, including type 1 diabetes (T1D),[4] has steadily been increasing in Europe and North America (2, 3). Therefore, both experimental and epidemiological data suggest that certain microorganisms will induce a state of protective tolerance in mammals toward autoimmune diseases such as T1D (4–6).

TLRs represent the early molecular sensors of invading microorganisms and link innate with adaptive immune responses (7–9). To date, 11 members of TLR have been identified in humans, and 13 in mice, and a series of genetic studies revealed their respective ligands. Mammalian TLRs can be expressed on the cell membrane (i.e., TLR1, TLR2, TLR5, and TLR6), intracellularly (TLR3, TLR7, TLR8, and TLR9), or both (TLR4). The distinct localization correlates with a different nature of stimulatory ligands—with transmembrane TLRs primarily sensing microbial membrane molecules, such as LPS and lipopeptides (TLR1, TLR2, TLR5, and TLR6), and intracellular forms recognizing microbial nucleic acids, such as CpG-containing DNA sequences (TLR9) and viral ssRNA (TLR7 and TLR8) or dsDNA (TLR3) (9), or a different signaling pathway (TLR4) (10).

The genetically diabetes-prone NOD mouse strain represents a prototypic experimental model of human T1D. In accordance with the principle of protective tolerance, decontamination of NOD mice from microbes does increase diabetes frequency. Conversely, deliberate infection of those mice with various microorganisms totally prevents diabetes onset if infection occurs early in life (5). An outstanding study has recently demonstrated that the interaction of intestinal microbes with the innate immune system is a critical epigenetic factor modifying T1D predisposition in NOD mice (11). Nonetheless, the precise mechanisms of induction of tolerance by the microbiota remain to be elucidated.

IDO is expressed in dendritic cells (DCs) in response to inflammatory stimuli, including IFN-γ and CpG oligodeoxynucleotide (ODN), and represents an important physiological mechanism capable of controlling both inflammation and autoimmunity (12–14). IDO catalyzes the first and rate-limiting step of tryptophan catabolism along the kynurenine pathway, which produces a series of tryptophan catabolites collectively known as kynurenines. We have previously demonstrated that IDO activity, hence, tryptophan catabolism, is not inducible by IFN-γ in DCs from NOD mice (15). This defect impairs tolerogenesis to a β cell-specific autoantigen also dominant in human T1D. Although maneuvers aimed at correcting the IDO defect will restore autoantigen-specific tolerogenesis (16), it is not currently known whether tryptophan catabolism plays a role in the development of the disease.

In the present study, we investigated whether TLRs and IDO are involved in the control of autoimmune diabetes in mice nongenetically prone to the disease. We found that both TLR9 and IDO are required for protection from an inflammatory/prodiabetic insult

Department of Experimental Medicine and Biochemical Sciences, University of Perugia, Perugia, Italy

Received for publication May 21, 2009. Accepted for publication September 7, 2009.

The costs of publication of this article were defrayed in part by the payment of page charges. This article must therefore be hereby marked *advertisement* in accordance with 18 U.S.C. Section 1734 solely to indicate this fact.

[1] This work was supported in part by the Associazione per l'Aiuto ai Giovani con Diabete dell'Umbria (to U.G.).

[2] F.F. and C.V. contributed equally to this work.

[3] Address correspondence and reprint requests to Dr. Ursula Grohmann, Department of Experimental Medicine and Biochemical Sciences, Via del Giochetto, 06126 Perugia, Italy. E-mail address: ugrohmann@tin.it

[4] Abbreviations used in this paper: T1D, type 1 diabetes; 1-MT, 1-methyl-DL-tryptophan; DC, dendritic cell; IKK, IκB kinase; ODN, oligodeoxynucleotide; pDC, plasmacytoid DC; PLN, pancreatic lymph node; SPF, specific pathogen free; STZ, streptozotocin; Treg, T regulatory; WT, wild type.

www.jimmunol.org/cgi/doi/10.4049/jimmunol.0901577

in healthy conditions. However, engagement of TLR9 by CpG-ODN did not efficiently induce IDO expression and activity in lymphoid tissues from NOD mice. Thus, our data: 1) confirm the protective role of TLRs in the prevention of T1D, 2) identify IDO as the critical TLR9 downstream effector in regulating inflammation/autoimmunity, and 3) suggest that successful prevention/therapy of T1D in genetically diabetes-prone subjects may require multiple and integrated approaches, capable of restoring an IDO-mediated, physiologically protective tolerance.

Materials and Methods

Mice

Four- and 8-wk-old C57BL/6 mice of either sex were obtained from Charles River Breeding Laboratories. Mice homozygous for the TLR3 (*Tlr3*$^{-/-}$) and TLR9 (*Tlr9*$^{-/-}$) targeted mutation raised on the C57BL/6 background were generated as described (17, 18), and bred at the breeding facilities of the University of Perugia. Female NOD/Mrk mice, 4 wk of age, were purchased from Taconic Farms. All animals were housed and fed under specific pathogen-free (SPF) conditions. All in vivo studies were in compliance with national (Italian Approved Animal Welfare Assurance A-3143-01) and Perugia University Animal Care and Use Committee guidelines.

In vivo treatments

For the induction of experimental autoimmune diabetes, wild-type (WT), *Tlr3*$^{-/-}$, or *Tlr9*$^{-/-}$ C57BL/6 mice were injected i.p. for 5 consecutive days with 40 mg/kg body weight of freshly made streptozotocin (STZ; Sigma-Aldrich) in 0.01 mol/L citrate buffer (pH 4.5). Day 1 was that of the first STZ injection. Control mice received vehicle alone. Nonfasting glucose levels in tail vein blood samples were monitored 1–2 times/wk. Mice with a blood glucose level of >250 mg/dl for ≥2 consecutive days were considered diabetic. To inhibit IDO activity in vivo, groups of WT mice were treated with slow-release pellets of 1-methyl-DL-tryptophan (1-MT; 150 mg/pellet, 7-day release at 0.9 mg/h) or placebo (both from Innovative Research of America) implanted on day 0 under the dorsal skin of the recipients, as described (19). In selected experiments, C57BL/6 WT mice were treated with 25 μg of CpG-ODN 1826 5′-TCCATGACGTTCCT GACGTT-3′ (custom, phosphorothioate; Invitrogen Life Technologies) on days 7 and 9, whereas 4-wk-old NOD mice received the same dose of CpG-ODN twice per week for 3 wk.

Histopathology and immunohistochemistry

Paraffin-embedded sections (3–4 μm) of pancreata (five per organ) were stained with H&E and analyzed by light microscopy. Insulitis scoring was according to the following criteria: severe insulitis (score 3), 50% or higher of the islet area is infiltrated; mild insulitis (score 2), <50% of the islet area is infiltrated; peri-insulitis (score 1), infiltration is restricted to the periphery of islets; and no insulitis (score 0), absence of cell infiltration. Results are presented as the percentage of islets per mouse in each category. At least 40 islets were counted per mouse blindly by two observers. In immunostaining for insulin, 4-μm sections were cut from paraffin blocks and captured on electrically charged slides (Sigma-Aldrich). Sections were dewaxed in zylene and stained with primary pig anti-mouse insulin Abs (DakoCytomation) for 1 h, washed in PBS, and incubated with goat anti-guinea pig tetramethyl rhodamine isothiocyanate conjugate for 45 min. Nuclei were counterstained with 4′,6-diamidino-2-phenylindole and mounted in 1,4-diazabicyclo[2.2.2]octane solution (all from Sigma-Aldrich). Slides were examined using a BX 41 apparatus in conjuction with F-View software (both from Olympus).

Cell isolation from pancreatic lymph nodes (PLNs) and peripheral lymphoid organs

Purification of CD4$^+$ T cells from pooled peripheral lymph nodes (with the exception of PLNs; see below) was conducted as described (20–22). For cytokine induction, cells (1×10^6/ml) were cultured in the presence of plate-bound anti-CD3ε (145-2C11) and anti-CD28 (PV-1) (both at the concentration of 1 μg/ml) for 48 h. Purification of PLN lymphocytes involved treating the organ with Complete Mini Protease inhibitors (Roche Applied Science), followed by digestion with collagenase type IV (Sigma-Aldrich) in the presence of bovine pancreatic DNase (Sigma-Aldrich) for 30 min at 37°C. The digested pancreata were further disrupted by gently pushing the tissue through a nylon screen, and pancreatic lymphocytes were separated on a Percoll gradient (Sigma-Aldrich). Purified PLN cells in STZ-treated mice (day 21) were made up of ~10% lymphocytes (mostly CD4$^+$), 3% monocytes, and 5% CD11c$^+$Ia$^+$ cells. In prediabetic NOD mice, the corresponding percentages were 16, 25, and 6%. Splenic DCs were purified by magnetic-activated sorting using CD11c MicroBeads and MidiMacs (Miltenyi Biotec), in the presence of EDTA to disrupt DC-T cell complexes, as described (15, 19). Cytokine production from PLN lymphocytes and splenic DCs was measured in culture supernatants harvested after 24-h cell incubation with medium alone. For the purification of plasmacytoid DCs (pDCs), CD11c$^+$ cells were further fractionated using mPDCA-1 MicroBeads (Miltenyi Biotec), as described (21).

Flow cytometry

In all FACS analyses, cells were treated with rat anti-CD16/32 (2.4G2) for 30 min at 4°C for blockade of Fc receptors before assaying on an EPICS flow cytometer using EXPO 32 ADC software (Beckman Coulter). CD4, CD25, CTLA-4, and CD62L expressions were analyzed as described (21). For intracellular Foxp3, cells were stained with anti-CD4 (GK1.5)-PE (BD Pharmingen), fixed, permeabilized, and stained with Alexa Fluor 488 anti-mouse Foxp3 (MF-14; Biolegend) or isotype control Alexa Fluor 488 rat IgG2b.

T regulatory (Treg) cell purification and suppression assay

CD4$^+$CD25$^+$ and CD4$^+$CD25$^-$ T cells were isolated from lymph nodes by MACS, as described (20, 23). The purity of either T cell fraction was more than 95%. For polyclonal Treg suppression assay, CD4$^+$CD25$^-$ cells were cocultured with irradiated T cell-depleted splenocyte samples and CD4$^+$CD25$^+$ cells for 3 days in the presence of soluble anti-CD3 (20, 23). Proliferation was measured by incorporation of [^{3}H]thymidine, according to standard procedures.

ELISA and TGF-β bioassay

Nonfasting blood insulin levels were measured by a mouse insulin ELISA kit (Mercodia AB). Cytokines (IL-2, IL-4, IL-6, IL-10, IL-17A, IL-23, and IFN-γ) were measured in culture supernatants by ELISA using specific kits or previously described reagents and procedures (21, 24). An ELISA-based TransAM Flexi NF-κB Family Kit (Active Motif) was used to monitor activity of NF-κB family members, as described (21, 24). Active TGF-β was measured, as described (25), using CCL-64 mink lung epithelial indicator cells (American Type Culture Collection), which do not appear to activate inactive TGF-β precursor molecules, but are extremely sensitive to growth inhibition induced by the biologically active cytokine.

Real-time PCR

Real-time PCR analysis was performed, as described (26), using *Ido1*-specific primers (S, 5′-GAAGGATCCTTGAAGACCAC-3′; AS, 5′-GAAGCTGC GATTTCCACCAA-3′). For all panels, bars represent the ratio of gene to *Gapdh* expression, as determined by the relative quantification method (ΔΔ cycle threshold; mean ± SD of triplicate determination).

Western blotting and IDO functional analysis

IDO expression was investigated in cells cultured overnight with complete medium either alone or in the presence of 1 μg/ml CpG-ODN by immunoblot with a rabbit anti-mouse IDO mAb raised in our laboratory (22). Anti-β-actin Ab (Sigma-Aldrich) was used as a normalizer. For measuring IDO functional activity, pDCs were stimulated either with 200 U/ml IFN-γ (R&D Systems) or 1 μg/ml CpG-ODN and, after 18 h, L-kynurenine, the main IDO product, was measured in culture supernatants by HPLC, as described (19). In PLN lymphocytes, treatment with IFN-γ, but not CpG-ODN, greatly reduced the cell viability, and thus, could not be used.

Nuclear extracts and EMSA

Nuclear extract preparation and EMSA were performed, as described (27). Briefly, DNA-binding reactions were conducted in 20 min at room temperature in a final volume of 20 μl. The reactions were started by adding 10 μg of nuclear protein extract to a reaction mix containing ~20,000 cpm of [γ-^{32}P]ATP-labeled NF-κB dsDNA ODN (5′-AGAGGGGACTTTC CGAGAGGC-3′) (27). Cold competitor ODN were added to the reaction mix before the radiolabeled probe (data not shown). For supershift experiments, protein extracts were incubated with anti-p65 or anti-RelB Ab (Santa Cruz Biotechnology) for 30 min at room temperature after the addition of the radiolabeled probe. Whole samples were then loaded on a 5% native polyacrylamide gel in Tris-borate-EDTA buffer.

Statistical analysis

In the in vivo experiments, glycemia data were analyzed by Kaplan-Meier plots. Paired data were evaluated by Student's *t* test. All in vitro determinations are means ± SD from at least three independent experiments, unless otherwise indicated. All *n* values were computed by power analysis, so as to yield a power of at least 80% with an α-level of 0.05.

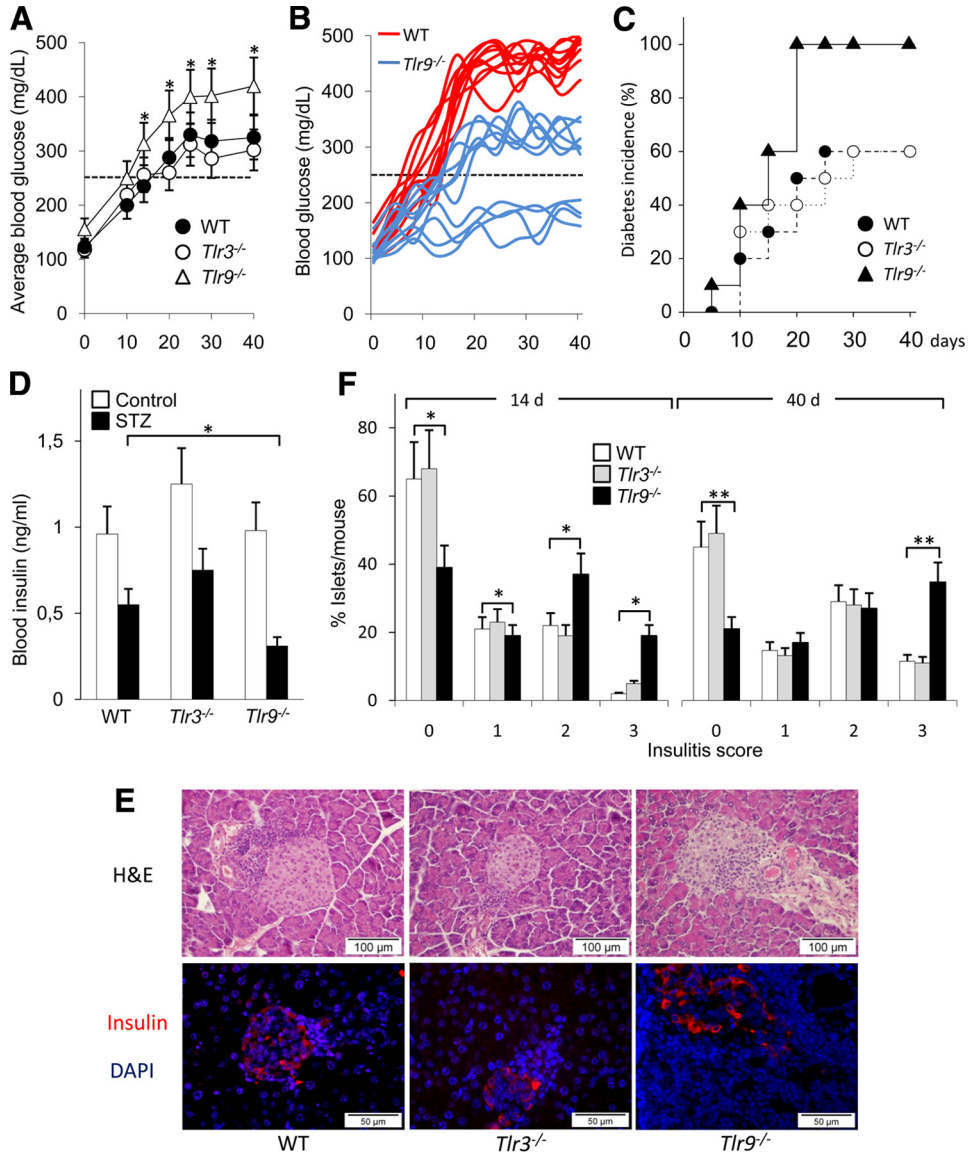

FIGURE 1. Higher susceptibility to STZ-induced diabetes in $Tlr9^{-/-}$ mice. WT ($n = 12$), $Tlr3^{-/-}$ ($n = 10$), and $Tlr9^{-/-}$ ($n = 10$) C57BL/6 mice were injected with STZ from day 1, and blood glucose was monitored over time (in *A–C*, one experiment is depicted of two with similar results). Diabetes was diagnosed in mice with blood glucose level >250 mg/dl. Mice were sacrificed at different times and analyzed for insulinemia (*D*) and pancreas histology (*E* and *F*) and immunohistochemistry (*E*). *A*, Average blood glucose in different groups is plotted over time. Data are presented as mean glucose levels ± SD. *, $p < 0.01$ ($Tlr9^{-/-}$ vs WT mice). *B*, Blood glucose concentrations over time in individual WT and $Tlr9^{-/-}$ mice. *C*, Incidence of diabetes over time in TLR-deficient and WT mice. $p < 0.01$ ($Tlr9^{-/-}$ vs WT mice). *D*, Blood insulin was measured by ELISA at day 30. Control, control animals treated with vehicle alone. Data are means ± SD of three experiments. *, $p < 0.05$ (STZ-treated $Tlr9^{-/-}$ vs WT mice). *E* and *F*, Pancreatic tissues were processed for H&E staining to evaluate insulitis (*E* and *F*) and immunostained for insulin (red, *E*). In fluorescent images, nuclei were counterstained with 4′,6-diamidino-2-phenylindole (blue). Representative islet area for each group (*E*) at day 40 and the percentages of islets per mouse with different score (*F*, see *Materials and Methods*) of lymphocyte infiltration (days 14 and 40) are shown. Percentages represented number of islets of a given score (see *Materials and Methods*) over total number of islets (30–40 per pancreas). *, $p < 0.01$ and **, $p < 0.001$ ($Tlr9^{-/-}$ vs WT mice).

Results

Tlr9$^{-/-}$ *mice are highly susceptible to experimental autoimmune diabetes*

To investigate the role of TLR3 and TLR9 in the pathogenesis of chemically induced autoimmune diabetes, we injected $Tlr3^{-/-}$ and $Tlr9^{-/-}$ mice and their C57BL/6 WT counterparts with multiple low doses of STZ. From 14 days, average were significantly higher in $Tlr9^{-/-}$, but not $Tlr3^{-/-}$ mice, as compared with WT animals, and further increased thereafter (Fig. 1*A*). In addition, whereas at least 40% WT and $Tlr3^{-/-}$ animals remained normoglycemic at day 40, all $Tlr9^{-/-}$ mice became diabetic as early as day 20 (Fig. 1, *B* and *C*). Although serum insulin levels were generally decreased in STZ-treated as compared with vehicle-injected counterparts, insulinemia in STZ-treated $Tlr9^{-/-}$ mice was significantly lower when compared with STZ-treated WT mice (Fig. 1*D*). Groups of mice injected with STZ were sacrificed at different times, and 5-μm-thick sections of pancreas were stained with H&E or immunostained for insulin. The majority of pancreatic islets of WT and $Tlr3^{-/-}$ mice were either normal or mildly infiltrated by leukocytes and clearly positive for insulin (Fig. 1*E*, day 40; Fig. 1*F*, days 14 and 40). In contrast, as much as 17% (at day 14) or 50% (at day 40) of the islets in $Tlr9^{-/-}$ mice were characterized by intrainsulitis and low insulin. Thus, our data suggest that $Tlr9^{-/-}$, but not $Tlr3^{-/-}$

Table I. *Quantitative analysis of T cell populations in gated CD4$^+$CD25$^+$ cells in spleens, lymph nodes, and PLNs in mice treated with STZ*[a]

Phenotype	Spleen						Lymph Nodes						PLNs					
	WT		*Tlr3*$^{-/-}$		*Tlr9*$^{-/-}$		WT		*Tlr3*$^{-/-}$		*Tlr9*$^{-/-}$		WT		*Tlr3*$^{-/-}$		*Tlr9*$^{-/-}$	
STZ	–	+	–	+	–	+	–	+	–	+	–	+	–	+	–	+	–	+
CTLA-4	27.8[a]	**41.3**	26.9	**39.7**	26.2	31.2	36.1	**46.9**	37.4	**48.5**	38.0	39.4	15.7	**28.9**	15.9	**29.9**	13.6	10.8
Foxp3	20.2	**28.2**	21.4	**28.8**	20.3	21.0	30.6	**39.7**	32.1	**44.3**	29.8	28.3	13.2	**19.4**	11.2	**20.1**	10.7	10.9
CD62L	ND	ND	ND	ND	ND	ND	25.1	21.3	23.6	22.8	24.2	23.2	ND	ND	ND	ND	ND	ND
CD4 CD25 (% in total cells)	7.5	8.3	6.9	8.0	7.6	8.9	8.1	9.2	7.8	8.9	8.5	9.5	12.1	13.8	10.6	12.7	13.3	14.9

[a] Data are mean percentages of positive cells of three experiments, each consisting of three mice per group per experiment. SD (not included in the table) never exceeded 10% of the mean value. Bold values, $p < 0.01$ (STZ treated vs untreated).

C57BL/6 mice develop an earlier and more severe form of experimental autoimmune diabetes than WT counterparts.

Lack of induction of Foxp3$^+$ Treg cells and higher production of proinflammatory IL-6 and IL-17A characterize diabetes in Tlr9$^{-/-}$ *mice*

Although Th1 cells appear to play a major role in autoimmune diabetes via IFN-γ production, discordant observations have been found on NOD mice expressing targeted mutations in either IFN-γ or its receptor (28–30). More recently, Th17 cells, clearly involved in many autoimmune diseases, such as experimental autoimmune encephalomyelitis, rheumatoid arthritis, and myocarditis, have been shown to promote pancreatic inflammation, although they induce diabetes efficiently in NOD/SCID mice only after conversion into Th1 cells (31, 32). In contrast, there is compelling evidence indicating that the development of diabetes in NOD mice is tightly controlled by Treg cells, via production of TGF-β and IL-10 (33). In experimental diabetes induced by STZ, the pattern of pathogenetic vs protective cells and cytokines is less clear, although administration of IL-23, a Th17-sustaining cytokine, greatly exacerbates the disease (34).

To examine whether TLR9 expression would affect the balance of Th and Treg responses in chemically induced diabetes, we used flow cytometry to evaluate the percentage and phenotype of CD4$^+$ T cells from lymphoid organs, i.e., spleen and lymph nodes, and PLN lymphocytes at day 21 of STZ treatment in WT, *Tlr3*$^{-/-}$, and *Tlr9*$^{-/-}$ mice. Mice injected with vehicle alone were used as a control. Table I shows that STZ treatment did not significantly modify the basal frequency of gated CD4$^+$CD25$^+$ T cells coexpressing the T cell activation marker CD62L in any groups. In contrast, the percentages of CD4$^+$CD25$^+$ T cells coexpressing either CTLA-4 or Foxp3, the Treg cell lineage transcription factor, significantly increased upon STZ treatment in samples from WT and *Tlr3*$^{-/-}$, but not *Tlr9*$^{-/-}$, mice. Foxp3 staining of CD4$^+$ T cells gated from lymph nodes further confirmed no significant modulation in CD4$^+$Foxp3$^+$ cells from TLR9-deficient mice treated with STZ (Fig. 2, *A* and *B*). However, although disparate in their occurrence, the suppressive activity of Treg cells purified from STZ-treated *Tlr9*$^{-/-}$ mice did not differ from that of Treg cells from diabetic WT or *Tlr3*$^{-/-}$ animals (Fig. 2*C*).

We next analyzed the pattern of Th1, Th2, Th17, and Treg-associated cytokine production by activated CD4$^+$ T cells purified from peripheral lymph nodes. In addition, cytokine production by CD11c$^+$ DCs purified from the spleen and by PLN lymphocytes, both types of cell under culture for 24 h without added stimuli, was also evaluated (Fig. 2*D*). In CD4$^+$ T cell cultures, we found that in vivo treatment with STZ induced a similar trend for the majority of the tested cytokines in both WT and TLR-deficient mice, with comparable increase in IL-2, IL-10, and TGF-β and a decrease in IFN-γ production, whereas IL-4 production was not modified. In contrast, the increase in IL-17A production in response to the drug was significantly higher in CD4$^+$ cell cultures from *Tlr9*$^{-/-}$, but not *Tlr3*$^{-/-}$ mice as compared with WT mice. In DC cultures, IL-23 increased equally in all STZ-treated groups, although a dramatic increase in IL-6 was found in supernatants from TLR9-deficient cells. In parallel, IL-6 and IL-17A levels were also significantly higher in PLN lymphocytes from STZ-treated *Tlr9*$^{-/-}$, but not *Tlr3*$^{-/-}$ mice, as compared with WT animals. Thus, our data suggest that lack of TLR9 expression may lead to a higher production of proinflammatory IL-6 in diabetic *Tlr9*$^{-/-}$ mice that, combined with high levels of IL-23, may impede the TGF-β-mediated expansion of Foxp3$^+$ Treg cells and skew the balance toward the development and differentiation of pathogenic Th17 cells.

IDO is not expressed in PLNs of diabetic Tlr9$^{-/-}$ *mice*

IDO has a primary role in the peripheral generation of Treg cells, under physiological or pathological conditions (14). Furthermore, in experimental pathogenic inflammation, IDO helps to tame overzealous and exaggerated inflammatory response driven by IL-23 and IL-17 (22). In contrast, these cytokines can down-regulate tryptophan catabolism (35, 36). Signaling through TLR9 induces IDO expression in splenic DCs, particularly in the plasmacytoid subset (pDC), and functional tryptophan catabolism is necessary for TLR9-driven immunosuppressive effects (14, 37). We therefore became interested in ascertaining whether a defect in IDO expression could be involved in the exacerbated disease induced by STZ in *Tlr9*$^{-/-}$ mice. To this purpose, we analyzed IDO expression and activity in both splenic pDCs and PLN cells purified from mice at day 21 of STZ treatment (Fig. 3). Mice injected with vehicle alone were used as control. We found that IDO transcript (Fig. 3*A*) and protein expression greatly increased in splenic pDCs upon in vivo STZ treatment of WT and *Tlr3*$^{-/-}$ mice, whereas in pDCs from animals lacking TLR9 the induction was barely detectable. In PLNs, IDO was expressed in samples from WT and *Tlr3*$^{-/-}$ mice and further increased following STZ treatment. In contrast, IDO expression could not be detected under basal conditions nor after in vivo treatment of *Tlr9*$^{-/-}$ mice with STZ (Fig. 3, *B* and *C*). IDO expression was accompanied by significant kynurenine production by splenic pDCs from WT and *Tlr3*$^{-/-}$ mice after in vivo treatment with STZ and further increased in response to in vitro restimulation with IFN-γ, whereas a significantly lower level of the tryptophan metabolite was present in parallel culture supernatants from *Tlr9*$^{-/-}$ pDCs, either untreated or treated with the cytokine (Fig. 3*D*). Thus, our data suggest that deficient TLR9 expression may determine defective IDO induction in response to pancreatic inflammation.

In vivo treatment with CpG-ODN protects mice from STZ-induced diabetes in an IDO-dependent fashion

To evaluate the functional role of IDO as induced in the course of diabetes development and its potential link with TLR9 activation, WT recipients were administered 1-MT, the gold standard in IDO

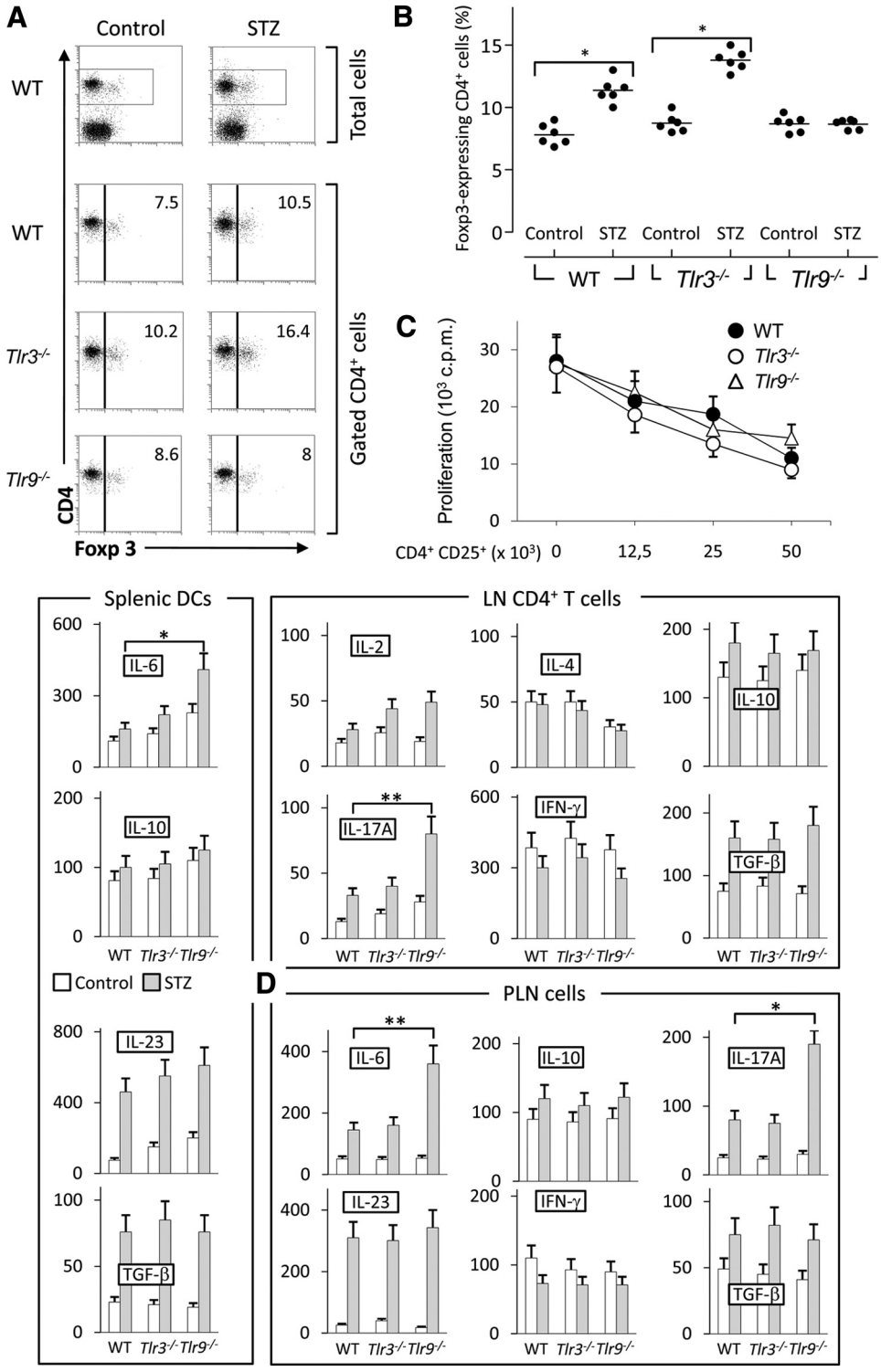

FIGURE 2. CD4/Foxp3 expression, Treg-suppressive activity, and cytokine production in diabetic *Tlr9*$^{-/-}$ mice. Groups of mice treated as in Fig. 1 were sacrificed at day 21. As controls, prospective recipients were treated with vehicle alone. *A*, *Upper part*, Representative FACS dot plots for CD4 and Foxp3 expression in permeabilized total lymph node cells from vehicle (control)- and STZ-injected WT animals are shown. *Lower part*, Dot plots for gated CD4 T cells. Numbers indicate the percentage of Foxp3 expression in gated CD4$^+$ cells. Number indicates percentage of double-positive cells. Data are representative of three experiments. *B*, The scattergram reflects the percentages of Foxp3-expressing CD4$^+$ cells in individual mice (n = 6). *, $p < 0.001$ (STZ-treated vs control mice). *C*, Cocultures of CD4$^+$CD25$^-$ cells (1×10^5) from naive WT mice were established with various numbers of CD4$^+$CD25$^+$ cells (horizontal axis) obtained from STZ-treated WT or TLR-deficient mice in the presence of soluble anti-CD3 Ab (1 μg/ml) and APCs. Data are means ± SD of triplicate samples and are from one experiment representative of three. *D*, CD4$^+$ T cells purified from pooled peripheral lymph nodes (LN) were cultured in the presence of plate-bound anti-CD3 and anti-CD28 and, after 48 h, supernatants were assayed for cytokine content by ELISA. TGF-β was quantified by either ELISA (data not shown) or bioassay with similar results. Cytokine production was also assessed in supernatants from splenic DCs and PLN cells cultured in medium alone for 24 h. Cytokine levels are expressed in pg/ml with the exception of IL-2, expressed in U/ml. Results are means ± SD of three experiments. *, $p < 0.01$ (STZ-treated *Tlr9*$^{-/-}$ vs WT mice).

inhibition, in the form of slow release pellets implanted on day 0, i.e., 1 day before STZ treatment. Control mice received placebo pellets. All mice treated with STZ and 1-MT developed hyperglycemia (Fig. 4, *A* and *B*) with a kinetic pattern comparable to that manifested by *Tlr9*$^{-/-}$ mice treated with STZ alone (Fig. 1*B*). Conversely, administration of CpG-ODN determined a reduced frequency of hyperglycemic animals, an effect that could be reversed by cotreatment with 1-MT, but not placebo pellets (Fig. 4*B*). The therapeutic effect of CpG-ODN was accompanied by a significant increase in the percentage of CD4$^+$Foxp3$^+$ cells in lymph nodes (>50% increase in three experiments; $p < 0.001$, CpG-ODN vs PBS), whereas the opposite pattern could be observed in mice treated with 1-MT, either alone or combined with CpG-ODN (>50% decrease in three experiments; $p < 0.001$, 1-MT vs prospective placebo) (Fig. 4*C*). In addition, IL-17A and IL-6/IL-23 productions by lymph node CD4$^+$ cells and by splenic DCs, respectively, further increased in mice treated with STZ and 1-MT ± CpG-ODN, but decreased after in vivo treatment with STZ in combination with CpG-ODN and placebo. In PLNs, CpG-ODN treatment significantly reduced the production of both IL-6 and IL-17A in an IDO-dependent fashion (Fig. 4*D*). Our data therefore indicate that an intact tryptophan catabolism is required

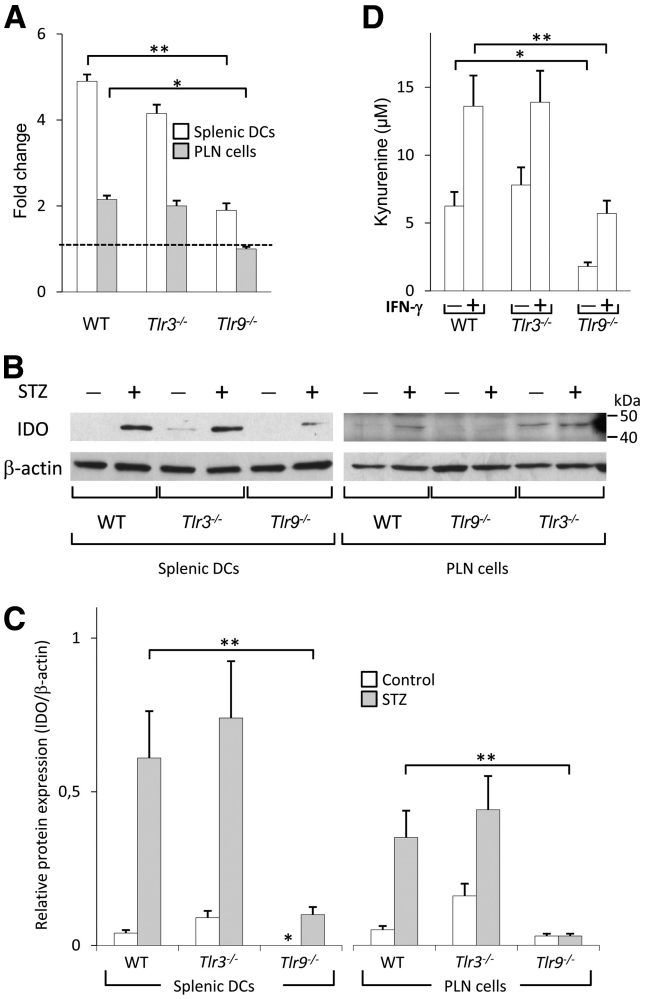

FIGURE 3. Lack of IDO induction in diabetic *Tlr9*$^{-/-}$ mice. Groups of mice treated with STZ as in Fig. 1 were sacrificed at day 21 and pDCs were purified from the spleen. Lymphocytes from PLNs were also harvested. *A*, mRNA levels of *Ido1* were quantified by real-time PCR using *Gapdh* normalization. Data (means ± SD of three experiments) are presented as normalized transcript expression in the samples (cells from STZ-treated mice) relative to normalized expression in the respective controls, i.e., cells from untreated mice (fold change = 1; dotted line). *B*, IDO protein expression was assayed by immunoblot analysis of whole-cell lysates. Blots were stripped and reprobed with anti-β-actin Ab. One of three experiments. *C*, Data obtained as in *B* (means ± SD from three experiments) were analyzed by scanning densitometry and are presented as IDO protein expression relative to β-actin. *, Undetectable IDO protein densitometric value. **, $p < 0.01$. *D*, Functional IDO activity was measured in terms of L-kynurenine levels in supernatants from splenic pDCs treated overnight with IFN-γ. Data are means ± SD of three experiments. *, $p < 0.01$ and **, $p < 0.001$.

for mitigating the inflammatory/diabetogenic effects of STZ in C57BL/6 mice, and that activation of TLR9 in vivo can protect from the pathogenic inflammatory response at the pancreas level in an IDO-dependent fashion.

CpG-ODN does not induce IDO expression and activity in PLNs of NOD mice

The NOD strain of mice has become a prototypic model of autoimmune diabetes (3). Most female mice die of hyperglycemia, reflecting the onset of insulitis at 4 wk of age and the consequent T cell-mediated destruction of pancreatic ß cells. The immune dysregulation in NOD mice has been ascribed to many causes, including aberrant APC function, reduced suppressive activity of Treg cells (38), and, more recently, resistance to regulation in T cell effectors (39). In 2003, our group provided the first evidence that IFN-γ fails to induce IDO, and hence, tolerizing properties in splenic DCs from NOD female mice early in prediabetes (15). Prompted by the results obtained in the STZ diabetes model, we administered multiple doses of CpG-ODN to 4-wk-old NOD females. No protection, but rather acceleration of diabetes development could be observed in CpG-ODN-treated mice as compared with vehicle-treated counterparts (Fig. 5, *A* and *B*), despite considerable expression of *Tlr9* transcripts in both splenocytes and PLN cells, which was comparable to that of C57BL/6 mice of same sex and age (data not shown). Lack of protection from diabetes was accompanied by very low induction of IDO expression in both splenic pDCs and PLN cells by in vitro incubation with CpG-ODN of cells from NOD as compared with STZ-treated C57BL/6 mice (Fig. 5, *C* and *D*). Accordingly, IDO activity was also poorly observed in the former cells (Fig. 5*E*). CpG-ODN, however, was capable of inducing high production of IL-6 in NOD PLNs as compared with parallel samples from C57BL/6 mice, either untreated or treated with STZ (Fig. 5*F*), in the face of basally higher levels of the cytokine. Because IL-6 can antagonize tryptophan catabolism via induction of proteasomal degradation of IDO (40), our data suggest that an aberrant TLR9 signaling producing high levels of IL-6 may underlie the exacerbating effects of CpG-ODN in NOD mice.

We have recently demonstrated that IDO expression is contingent on the noncanonical pathway of NF-κB activation (14, 21, 26). Recent molecular dissection of NF-κB activation has shown that NF-κB can be induced by the so-called canonical (classical) and noncanonical (alternative) signaling pathways, leading to distinct patterns in the individual NF-κB subunits that are activated and the downstream genetic responses that are induced. The proinflammatory canonical pathway involves activation of the IκB kinase (IKK)-β, which leads to phosphorylation-induced proteolysis of the inhibitor IκBα and consequent nuclear translocation of the p65 subunit in the form of p50-p65 dimers. In the noncanonical pathway, activation of IKKα by NF-κB-inducing kinase results in the processing of p100 to p52 and consequent formation of p52-RelB dimers, which translocate into the nucleus and activate an anti-inflammatory gene program (13, 14). In pDCs, triggering of TLR9 can activate both IKKα- and IKKβ-mediated pathways (41). To investigate whether the inability of CpG-ODN to induce IDO in NOD mice could be due to altered signaling, PLN lymphocytes from both WT C57BL/6 and NOD mice were stimulated in vitro with CpG-ODN and, after 30–60 min, NF-κB family activation was quantified by means of an ELISA kit specific for p65 and p52 (Fig. 5*G*). In WT C57BL/6 cells, either untreated or treated with STZ, we found that CpG-ODN activated nuclear translocation of p65 and p52 to a similar extent. In contrast, in NOD cells, the nuclear translocation of p65 was significantly higher than that of p52 as early as at 30 min, suggesting the occurrence of a dominant, proinflammatory response mediated by canonical NF-κB in NOD immune cells upon engagement of TLR9. The preferential activation of p65 in NOD PLN cells in response to TLR9 stimulation was further confirmed by EMSA (Fig. 5*H*).

Discussion

IDO is a metabolic enzyme conserved through the last 600 million years of evolution. Initially confined to the regulation of tryptophan availability in local tissue microenvironments, IDO is now considered to play a wider role, which extends to homeostasis and plasticity of the immune system, with implications for many aspects of immunopathology, including chronic inflammation and

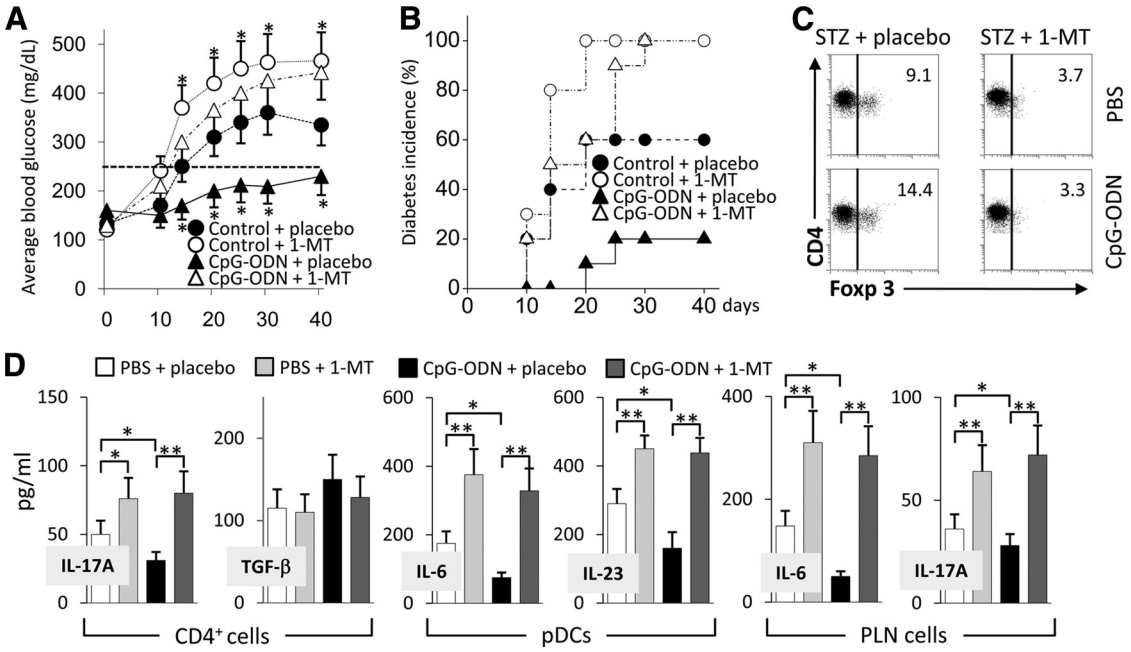

FIGURE 4. IDO-dependent protection by CpG-ODN from STZ-induced diabetes. Groups of WT mice ($n = 10$) were treated with STZ alone (days 1–5) or in combination with CpG-ODN (days 7 and 9) and/or 1-MT (day 0). Controls received STZ, PBS (days 7 and 9), and placebo pellets (day 0). *A* and *B*, Blood glucose levels were monitored over time, and average blood glucose (*A*) and diabetes incidence (*B*) were plotted over time, as in Fig. 1. *B*, $p < 0.05$ (PBS + 1-MT or CpG-ODN + placebo vs control + placebo) and $p < 0.001$ (CpG-ODN + 1-MT vs CpG-ODN + placebo). Parallel groups of mice were sacrificed at day 21 and analyzed for expression of Foxp3 in gated $CD4^+$ cells (*C*) and cytokine production (*D*), as in Fig. 2. $CD4^+$ T cells were purified from pooled peripheral lymph nodes and pDCs from spleens. PLN cells were also assayed. *A–C*, One experiment is shown of three. *D*, Data (pg/ml) are means ± SD of three experiments.

autoimmunity (14). Its immunoregulatory effects are mainly mediated by DCs and involve not only tryptophan deprivation, but also the production of kynurenines, which act on IDO^- DCs, thus rendering an otherwise stimulatory DC capable of regulatory effects (42), as well as on T cells. As a result, IDO^+ DCs mediate multiple effects on T lymphocytes, including inhibition of proliferation, apoptosis, and differentiation toward a regulatory phenotype (12–14). In addition to much evidence substantiating a critical role for tryptophan catabolism in immune regulation at the DC/T cell level, nonimmune cells such as pancreatic β cells from healthy patients as well as other islet cells will express the enzyme in response to IFN-γ (43). Furthermore, transfection of *Ido1*, the gene coding for mouse IDO, into β cells prolongs graft survival in NOD mice (44). Thus, in inflammatory conditions, an effective tryptophan catabolism at the pancreatic level may participate in islet protection in individuals nongenetically prone to autoimmune diabetes.

TLRs play a central role in the generation of innate and adaptive antimicrobial immune responses through recognition of conserved pathogen-associated molecular patterns. The majority of TLRs signal through the MyD88 adaptor protein, except for TLR4 and TLR3, which can or must signal by means of TIR domain-containing adaptor inducing IFN-β (7–9). After proper elimination of the invading microorganisms, anti-inflammatory signals are necessary for the restoration of the homeostatic balance, and hence, host protection from the deleterious effects of overwhelming inflammation. TLR signaling is involved not only in the primary induction of inflammation, but also in secondary regulatory mechanisms (6, 45, 46). Among these, IDO may represent the downstream effector for at least some TLRs, including the nucleic acid-binding TLR3 and TLR9. Although the TLR3 ligand poly(I:C) can induce IDO in nonimmune cells such as astrocytes (47) and gingival fibroblasts (48), CpG-ODN is known to induce the enzyme activity in immune cells, particularly pDCs, promoting strong immunoregulatory effects (37, 49–51).

Because of the crucial role of IDO in immune tolerance and the possible link between tryptophan catabolism and protective tolerance by pathogen-associated molecular patterns (6), we sought to examine whether TLR3 and TLR9 could play a role in the control of autoimmune diabetes and whether IDO would be involved in such effects. To this purpose, we examined experimental diabetes as induced by multiple low doses of STZ. Although not extensively characterized, this model is widely considered autoimmune in nature, because disease is prevented by administration of anti-T cell mAb and can be adoptively transferred using splenocytes from diabetic animals. Furthermore, the overt disease is preceded by islet inflammation, characterized by infiltration of immune cells as early as 3–4 days after the last STZ injection (52).

We found that hyperglycemia was induced in ~60% of WT C57BL/6 mice by STZ and was accompanied by significantly reduced insulinemia, mild islet infiltration, and a cytokine pattern dominated by IL-6, IL-23, TGF-β, and IL-17A, suggesting the occurrence of a Th17-mediated response. However, the increased number of T cells with a regulatory phenotype ($CD4^+Foxp3^+$) in peripheral lymphoid organs and in pancreas-associated lymphoid tissue, in addition to the high level of TGF-β produced by activated $CD4^+$ T cells, indicates the existence of counterregulatory mechanisms possibly acting to dampen the potent inflammatory effects of STZ. Although both receptors are potentially capable of transducing IDO-activating signals, TLR9- but not TLR3-deficient mice manifested an exacerbated diabetic syndrome. Lack of TLR9 determined an earlier appearance of hyperglycemia in all animals and a higher percentage of infiltrated islets, events accompanied by a lack of induction of $CD4^+Foxp3^+$ Treg cells in lymphoid organs and pancreata. In addition, the production of proinflammatory IL-6

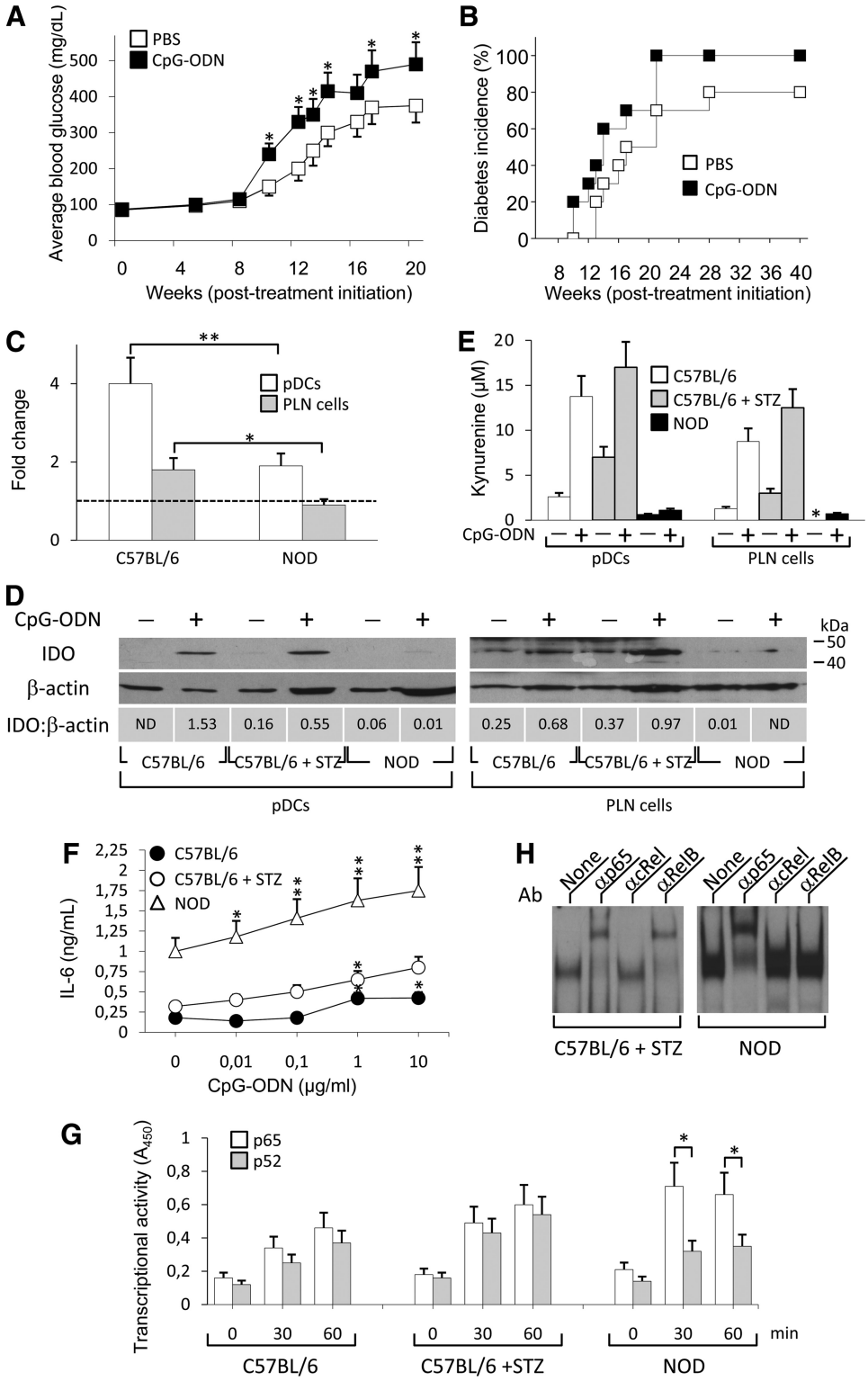

FIGURE 5. Lack of IDO and high IL-6 induction by CpG-ODN in PLNs of NOD mice. Four-week-old female NOD mice ($n = 10$) received 25 μg of CpG-ODN or PBS twice per week for 3 wk, and average blood glucose (*A*) and diabetes incidence (*B*) were plotted over time. *A* and *B*, $p < 0.05$ for comparison between the CpG-ODN-treated and control group. *C* and *D*, Purified splenic pDCs and PLN lymphocytes were purified from untreated 4-wk-old female NOD and STZ-treated C57BL/6 mice (day 21) and incubated with 1 μg/ml CpG-ODN overnight. Control cultures were obtained with medium alone. Transcripts and protein cell lysates were analyzed for IDO expression by real-time PCR (*C*) and immunoblot analysis (*D*), respectively, as in Fig. 3. *D*, The IDO to β-actin ratio, as determined by scanning densitometry, is indicated for each sample. *E*, IDO activity was measured in cell supernatants, as in Fig. 3*D*. Cells from untreated WT mice were also included in the assay. *, Undetectable level of kynurenine. *F*, IL-6 production was evaluated in supernatants from PLN cells incubated overnight with different doses of CpG-ODN by ELISA. *, $p < 0.001$ (CpG-ODN-treated vs respective untreated control). *C*, *E*, and *F*, Data are means ± SD of three experiments. *D*, One of three experiments is shown. *G*, PLN cells from NOD and C57BL/6 mice, the latter being untreated or treated with STZ, as in *E*, were stimulated with 1 μg/ml CpG-ODN and, after 30–60 min, p65 and p52 were quantified in nuclear extracts by means of a specific ELISA. Time 0 indicates untreated cells. Relative activities (A_{450}) are mean ± SD of three experiments, each in triplicate. *, $p < 0.01$. *H*, Nuclear extracts from PLN cells treated with CpG-ODN for 60 min were incubated with Ab against p65 or RelB. NF-κB dsDNA oligonucleotide was used as a probe. One of two experiments with the same results.

and IL-17A by immune cells deriving from both peripheral lymphoid tissues and PLNs was greatly increased in those mice in response to STZ, as compared with WT C57BL/6 counterparts. In PLNs, no or very low IDO protein and activity was to be detected in *Tlr9*$^{-/-}$ nondiabetic and diabetic mice, despite detectable basal enzyme expression and further induction in *Tlr3*$^{-/-}$ and WT animals by STZ in vivo treatment. In addition to substantiating and further defining the inflammatory/immunological aspects of STZ-induced diabetes, our data suggest that TLR9, but not TLR3 signaling, is necessary for the control of the disease and also for the induction of IDO at the pancreatic level.

The possible protective role of IDO was further investigated in WT mice by means of administration of either the IDO inhibitor 1-MT (which determined a more robust diabetic disease in response to STZ comparable to that of *Tlr9*$^{-/-}$ mice) or the TLR9 ligand CpG-ODN (which largely prevented hyperglycemia onset on condition that IDO was fully active). In the latter case, the TLR9-driven protection was accompanied by a further increase in

$CD4^+Foxp3^+$ Treg cells as compared with controls, whereas production of proinflammatory IL-6 and IL-17A from PLN lymphocytes was reduced. Therefore, our data further extend the protective potential of the TLR9-IDO axis from animal models of allergic disorders (14) to experimental autoimmune diabetes induced in mice nongenetically prone to the disease, and reveal an essential role of IDO expression in PLNs for the control of insulitis and hyperglycemia. Interestingly, this axis is already known to be important in the generation of human adaptive Treg cells (53), whereas either CpG-ODN (54) or kynurenines (36, 55) can control Th17-mediated inflammatory responses in murine disease models. Although TLR9 and IDO have not been directly linked yet, it is interesting to note that experimental autoimmune encephalomyelitis can be exacerbated by either lack of TLR9 expression (56) or of IDO activity (57).

However, in the NOD mouse, the situation is far more complex. Wong et al. (58) provided evidence that the incidence of diabetes in *Tlr9*$^{-/-}$, but not *Tlr3*$^{-/-}$ NOD mice maintained in SPF conditions is significantly lower when compared with their heterozygous (*Tlr9*$^{+/-}$) littermates. In addition, Wen's group (11) demonstrated that NOD mice lacking MyD88, but not TLR3, exhibit loss of diabetes development when maintained in SPF conditions, despite the development of robust diabetes in a germfree environment. However, colonization of germfree *MyD88*$^{-/-}$ NOD mice with a defined microbial consortium attenuates the disease (11). Overall, the bulk of available data suggests that, in the NOD mouse, TLR9-MyD88 signaling does not protect against, but rather sustains pathogenesis. Nonetheless, alternative microbial signals, apparently not engaging TLR3, can exert protective effects. Paradoxically, STZ treatment both prevents and reverts islet destructive autoimmunity in NOD mice (59). Considering that TLR9 can be activated also by host unmethylated CpG-containing DNA and non-CpG DNA (46) and that STZ can induce multiple DNA modifications, it might be speculated that the STZ treatment is capable of generating endogenous, regulatory TLR9 ligands. In agreement with data from knockout NOD animals, our current data indicate that multiple i.p. injections of SPF NOD mice with CpG-ODN accelerate diabetes development. However, it has been previously reported that i.m. vaccination of SPF NOD mice with CpG-ODN significantly reduces the incidence of diabetes (60). Although s.c. vs i.v. CpG-ODN administration has already been shown to determine opposite effects (50), it is worth mentioning that the successful i.m. administration of CpG-ODN was preceded by the injection of cardiotoxin, a molecular adjuvant particularly effective in i.m. DNA vaccinations. In this specific case, cardiotoxin pretreatment may have reset the dysregulated immune system of the NOD mouse (38), allowing CpG-ODN to exert an effective immunosuppressive effect. Thus, the inability of TLR9 to induce a regulatory pathway in NOD mice may rely on the absence of appropriate endogenous TLR9 ligands and/or the existence of signaling defects.

In evaluating the capacity of individual TLRs to promote either inflammation/autoimmunity or protective tolerance, the dominance of specific signaling pathways should be taken into account (46). TLR9 is known to signal via the MyD88 adapter, which, in pDCs, can activate two distinct NF-κB pathways, namely the classical or canonical pathway (in which IKKβ kinase plays a pivotal role) and the alternative or noncanonical pathway (which relies on IKKα activation). Although TLR9-IKKβ signaling leads to the nuclear translocation of p50-p65 dimers and production of classical proinflammatory cytokines, activation of IKKα by TLR9 triggering induces type I IFNs via nuclear translocation of p52-RelB complexes (41). We have recently found that noncanonical NF-κB activation is necessary for the induction of IDO-mediated therapeutic effects in a model of airway allergic inflammation (21). Furthermore, type I IFNs, although less potent than IFN-γ, can also act as IDO inducers (13, 14). Our current data indicate that the CpG-ODN treatment, either in vivo (data not shown) or in vitro, does not induce IDO protein and activity in NOD splenic pDCs and PLNs, despite a considerable induction in parallel samples from diabetic WT C57BL/6 mice. Lack of IDO induction is accompanied by overactivation of the proinflammatory p65 as compared with anti-inflammatory p52 subunit, whereas in cells from diabetic and nondiabetic C57BL/6 mice the amounts of p65 and p52 activated by CpG-ODN are quite similar. Although we cannot presently exclude the absence of appropriate TLR9 ligands, our data indicate that a dysfunctional TLR9 signaling may underlie the pathogenic/proinflammatory effect of this receptor in spontaneous autoimmune diabetes and may impede the effective induction of counterregulatory mechanisms mediated by IDO.

In conclusion, the identification of the molecular targets and mechanisms through which microbial ligands exert their protective effects may lead to a better understanding of the early pathogenesis processes involved in T1D, may provide new markers for an early diagnosis of the disease, and can ultimately lead to the generation of drugs mimicking protective microbial entities that can be used in either the prevention and/or treatment of T1D patients. The present study suggests that activation of TLR9, but not TLR3, can induce IDO, and thus control early inflammatory attacks to β cells. Harmonious TLR9 signaling, however, seems to be mandatory for fully protective activity of tryptophan catabolism. The latter, indeed, appears to be defective not only systematically, but also specifically in pancreas-associated lymph nodes of NOD mice. Thus, TLR9 and IDO may represent innovative and valuable molecular targets in the prevention/therapy of T1D. Although we are still currently evaluating the existence of a possible IDO defect in T1D patients, our data support the recent hypothesis that only combination therapies, capable of correcting the dysregulated immune signaling at multiple levels, will enable the permanent prevention and curing of T1D (61).

Acknowledgments

We thank G. Andrielli for technical assistance and digital art.

Disclosures

The authors have no financial conflict of interest.

References

1. Feleszko, W., J. Jaworska, and E. Hamelmann. 2006. Toll-like receptors: novel targets in allergic airway disease (probiotics, friends and relatives). *Eur. J. Pharmacol.* 533: 308–318.
2. Gale, E. A. 2002. The rise of childhood type 1 diabetes in the 20th century. *Diabetes* 51: 3353–3361.
3. Bach, J. F. 2002. The effect of infections on susceptibility to autoimmune and allergic diseases. *N. Engl. J. Med.* 347: 911–920.
4. Strachan, D. P. 1989. Hay fever, hygiene, and household size. *B.M.J.* 299: 1259–1260.
5. Bach, J. F. 2005. Infections and autoimmune diseases. *J. Autoimmun.* 25(Suppl.): 74–80.
6. Romani, L., and P. Puccetti. 2006. Protective tolerance to fungi: the role of IL-10 and tryptophan catabolism. *Trends Microbiol.* 14: 183–189.
7. Medzhitov, R. 2001. Toll-like receptors and innate immunity. *Nat. Rev. Immunol.* 1: 135–145.
8. Iwasaki, A., and R. Medzhitov. 2004. Toll-like receptor control of the adaptive immune responses. *Nat. Immunol.* 5: 987–995.
9. Akira, S., S. Uematsu, and O. Takeuchi. 2006. Pathogen recognition and innate immunity. *Cell* 124: 783–801.
10. Kagan, J. C., T. Su, T. Horng, A. Chow, S. Akira, and R. Medzhitov. 2008. TRAM couples endocytosis of Toll-like receptor 4 to the induction of interferon-β. *Nat. Immunol.* 9: 361–368.
11. Wen, L., R. E. Ley, P. Y. Volchkov, P. B. Stranges, L. Avanesyan, A. C. Stonebraker, C. Hu, F. S. Wong, G. L. Szot, J. A. Bluestone, et al. 2008. Innate immunity and intestinal microbiota in the development of type 1 diabetes. *Nature* 455: 1109–1113.
12. Grohmann, U., F. Fallarino, and P. Puccetti. 2003. Tolerance, DCs and tryptophan: much ado about IDO. *Trends Immunol.* 24: 242–248.

13. Mellor, A. L., and D. H. Munn. 2004. IDO expression by dendritic cells: tolerance and tryptophan catabolism. *Nat. Rev. Immunol.* 4: 762–774.
14. Puccetti, P., and U. Grohmann. 2007. IDO and regulatory T cells: a role for reverse signalling and non-canonical NF-κB activation. *Nat. Rev. Immunol.* 7: 817–823.
15. Grohmann, U., F. Fallarino, R. Bianchi, C. Orabona, C. Vacca, M. C. Fioretti, and P. Puccetti. 2003. A defect in tryptophan catabolism impairs tolerance in nonobese diabetic mice. *J. Exp. Med.* 198: 153–160.
16. Fallarino, F., R. Bianchi, C. Orabona, C. Vacca, M. L. Belladonna, M. C. Fioretti, D. V. Serreze, U. Grohmann, and P. Puccetti. 2004. CTLA-4-Ig activates forkhead transcription factors and protects dendritic cells from oxidative stress in nonobese diabetic mice. *J. Exp. Med.* 200: 1051–1062.
17. Heer, A. K., A. Shamshiev, A. Donda, S. Uematsu, S. Akira, M. Kopf, and B. J. Marsland. 2007. TLR signaling fine-tunes anti-influenza B cell responses without regulating effector T cell responses. *J. Immunol.* 178: 2182–2191.
18. Romani, L., F. Bistoni, K. Perruccio, C. Montagnoli, R. Gaziano, S. Bozza, P. Bonifazi, G. Bistoni, G. Rasi, A. Velardi, et al. 2006. Thymosin α1 activates dendritic cell tryptophan catabolism and establishes a regulatory environment for balance of inflammation and tolerance. *Blood* 108: 2265–2274.
19. Grohmann, U., C. Orabona, F. Fallarino, C. Vacca, F. Calcinaro, A. Falorni, P. Candeloro, M. L. Belladonna, R. Bianchi, M. C. Fioretti, and P. Puccetti. 2002. CTLA-4-Ig regulates tryptophan catabolism in vivo. *Nat. Immunol.* 3: 1097–1101.
20. Fallarino, F., U. Grohmann, S. You, B. C. McGrath, D. R. Cavener, C. Vacca, C. Orabona, R. Bianchi, M. L. Belladonna, C. Volpi, et al. 2006. The combined effects of tryptophan starvation and tryptophan catabolites down-regulate T cell receptor ζ-chain and induce a regulatory phenotype in naive T cells. *J. Immunol.* 176: 6752–6761.
21. Grohmann, U., C. Volpi, F. Fallarino, S. Bozza, R. Bianchi, C. Vacca, C. Orabona, M. L. Belladonna, E. Ayroldi, G. Nocentini, et al. 2007. Reverse signaling through GITR ligand enables dexamethasone to activate IDO in allergy. *Nat. Med.* 13: 579–586.
22. Romani, L., F. Fallarino, A. De Luca, C. Montagnoli, C. D'Angelo, T. Zelante, C. Vacca, F. Bistoni, M. C. Fioretti, U. Grohmann, et al. 2008. Defective tryptophan catabolism underlies inflammation in mouse chronic granulomatous disease. *Nature* 451: 211–215.
23. Orabona, C., U. Grohmann, M. L. Belladonna, F. Fallarino, C. Vacca, R. Bianchi, S. Bozza, C. Volpi, B. L. Salomon, M. C. Fioretti, et al. 2004. CD28 induces immunostimulatory signals in dendritic cells via CD80 and CD86. *Nat. Immunol.* 5: 1134–1142.
24. Montagnoli, C., F. Fallarino, R. Gaziano, S. Bozza, S. Bellocchio, T. Zelante, W. P. Kurup, L. Pitzurra, P. Puccetti, and L. Romani. 2006. Immunity and tolerance to *Aspergillus* involve functionally distinct regulatory T cells and tryptophan catabolism. *J. Immunol.* 176: 1712–1723.
25. Spaccapelo, R., L. Romani, L. Tonnetti, E. Cenci, A. Mencacci, G. Del Sero, R. Tognellini, S. G. Reed, P. Puccetti, and F. Bistoni. 1995. TGF-β is important in determining the in vivo patterns of susceptibility or resistance in mice infected with *Candida albicans*. *J. Immunol.* 155: 1349–1360.
26. Belladonna, M. L., C. Volpi, R. Bianchi, C. Vacca, C. Orabona, M. T. Pallotta, L. Boon, S. Gizzi, M. C. Fioretti, U. Grohmann, and P. Puccetti. 2008. Cutting edge: autocrine TGF-β sustains default tolerogenesis by IDO-competent dendritic cells. *J. Immunol.* 181: 5194–5198.
27. Grohmann, U., M. L. Belladonna, R. Bianchi, C. Orabona, E. Ayroldi, M. C. Fioretti, and P. Puccetti. 1998. IL-12 acts directly on DC to promote nuclear localization of NF-κB and primes DC for IL-12 production. *Immunity* 9: 315–323.
28. Wang, B., I. Andre, A. Gonzalez, J. D. Katz, M. Aguet, C. Benoist, and D. Mathis. 1997. Interferon-γ impacts at multiple points during the progression of autoimmune diabetes. *Proc. Natl. Acad. Sci. USA* 94: 13844–13849.
29. Hultgren, B., X. Huang, N. Dybdal, and T. A. Stewart. 1996. Genetic absence of γ-interferon delays but does not prevent diabetes in NOD mice. *Diabetes* 45: 812–817.
30. Serreze, D. V., C. M. Post, H. D. Chapman, E. A. Johnson, B. Lu, and P. B. Rothman. 2000. Interferon-γ receptor signaling is dispensable in the development of autoimmune type 1 diabetes in NOD mice. *Diabetes* 49: 2007–2011.
31. Martin-Orozco, N., Y. Chung, S. H. Chang, Y. H. Wang, and C. Dong. 2009. Th17 cells promote pancreatic inflammation but only induce diabetes efficiently in lymphopenic hosts after conversion into Th1 cells. *Eur. J. Immunol.* 39: 216–224.
32. Bending, D., H. De La Pena, M. Veldhoen, J. M. Phillips, C. Uyttenhove, B. Stockinger, and A. Cooke. 2009. Highly purified Th17 cells from BDC2.5NOD mice convert into Th1-like cells in NOD/SCID recipient mice. *J. Clin. Invest.* 119: 565–572.
33. You, S., M. A. Alyanakian, B. Segovia, D. Damotte, J. Bluestone, J. F. Bach, and L. Chatenoud. 2008. Immunoregulatory pathways controlling progression of autoimmunity in NOD mice. *Ann. NY Acad. Sci.* 1150: 300–310.
34. Mensah-Brown, E. P., A. Shahin, M. Al-Shamisi, X. Wei, and M. L. Lukic. 2006. IL-23 leads to diabetes induction after subdiabetogenic treatment with multiple low doses of streptozotocin. *Eur. J. Immunol.* 36: 216–223.
35. Zelante, T., A. De Luca, P. Bonifazi, C. Montagnoli, S. Bozza, S. Moretti, M. L. Belladonna, C. Vacca, C. Conte, P. Mosci, et al. 2007. IL-23 and the Th17 pathway promote inflammation and impair antifungal immune resistance. *Eur. J. Immunol.* 37: 2695–2706.
36. Romani, L., T. Zelante, A. De Luca, F. Fallarino, and P. Puccetti. 2008. IL-17 and therapeutic kynurenines in pathogenic inflammation to fungi. *J. Immunol.* 180: 5157–5162.
37. Fallarino, F., C. Orabona, C. Vacca, R. Bianchi, S. Gizzi, C. Asselin-Paturel, M. C. Fioretti, G. Trinchieri, U. Grohmann, and P. Puccetti. 2005. Ligand and cytokine dependence of the immunosuppressive pathway of tryptophan catabolism in plasmacytoid dendritic cells. *Int. Immunol.* 17: 1429–1438.
38. Delovitch, T. L., and B. Singh. 1997. The nonobese diabetic mouse as a model of autoimmune diabetes: immune dysregulation gets the NOD. *Immunity* 7: 727–738.
39. D'Alise, A. M., V. Auyeung, M. Feuerer, J. Nishio, J. Fontenot, C. Benoist, and D. Mathis. 2008. The defect in T-cell regulation in NOD mice is an effect on the T-cell effectors. *Proc. Natl. Acad. Sci. USA* 105: 19857–19862.
40. Orabona, C., M. T. Pallotta, C. Volpi, F. Fallarino, C. Vacca, R. Bianchi, M. L. Belladonna, M. C. Fioretti, U. Grohmann, and P. Puccetti. 2008. SOCS3 drives proteasomal degradation of indoleamine 2,3-dioxygenase (IDO) and antagonizes IDO-dependent tolerogenesis. *Proc. Natl. Acad. Sci. USA* 105: 20828–20833.
41. Kaisho, T., and T. Tanaka. 2008. Turning NF-κB and IRFs on and off in DC. *Trends Immunol.* 29: 329–336.
42. Belladonna, M. L., U. Grohmann, P. Guidetti, C. Volpi, R. Bianchi, M. C. Fioretti, R. Schwarcz, F. Fallarino, and P. Puccetti. 2006. Kynurenine pathway enzymes in dendritic cells initiate tolerogenesis in the absence of functional IDO. *J. Immunol.* 177: 130–137.
43. Sarkar, S. A., R. Wong, S. I. Hackl, O. Moua, R. G. Gill, A. Wiseman, H. W. Davidson, and J. C. Hutton. 2007. Induction of indoleamine 2,3-dioxygenase by interferon-γ in human islets. *Diabetes* 56: 72–79.
44. Alexander, A. M., M. Crawford, S. Bertera, W. A. Rudert, O. Takikawa, P. D. Robbins, and M. Trucco. 2002. Indoleamine 2,3-dioxygenase expression in transplanted NOD islets prolongs graft survival after adoptive transfer of diabetogenic splenocytes. *Diabetes* 51: 356–365.
45. Netea, M. G., J. W. Van der Meer, and B. J. Kullberg. 2004. Toll-like receptors as an escape mechanism from the host defense. *Trends Microbiol.* 12: 484–488.
46. Ehlers, M., and J. V. Ravetch. 2007. Opposing effects of Toll-like receptor stimulation induce autoimmunity or tolerance. *Trends Immunol.* 28: 74–79.
47. Suh, H. S., M. L. Zhao, M. Rivieccio, S. Choi, E. Connolly, Y. Zhao, O. Takikawa, C. F. Brosnan, and S. C. Lee. 2007. Astrocyte indoleamine 2,3-dioxygenase is induced by the TLR3 ligand poly(I:C): mechanism of induction and role in antiviral response. *J. Virol.* 81: 9838–9850.
48. Mahanonda, R., N. Sa-Ard-Iam, P. Montreekachon, A. Pimkhaokham, K. Yongvanichit, M. M. Fukuda, and S. Pichyangkul. 2007. IL-8 and IDO expression by human gingival fibroblasts via TLRs. *J. Immunol.* 178: 1151–1157.
49. Mellor, A. L., B. Baban, P. R. Chandler, A. Manlapat, D. J. Kahler, and D. H. Munn. 2005. Cutting edge: CpG oligonucleotides induce splenic $CD19^+$ dendritic cells to acquire potent indoleamine 2,3-dioxygenase-dependent T cell regulatory functions via IFN type 1 signaling. *J. Immunol.* 175: 5601–5605.
50. Wingender, G., N. Garbi, B. Schumak, F. Jungerkes, E. Endl, D. von Bubnoff, J. Steitz, J. Striegler, G. Moldenhauer, T. Tuting, et al. 2006. Systemic application of CpG-rich DNA suppresses adaptive T cell immunity via induction of IDO. *Eur. J. Immunol.* 36: 12–20.
51. Fallarino, F., and P. Puccetti. 2006. Toll-like receptor 9-mediated induction of the immunosuppressive pathway of tryptophan catabolism. *Eur. J. Immunol.* 36: 8–11.
52. Kim, Y. T., and C. Steinberg. 1984. Immunologic studies on the induction of diabetes in experimental animals: cellular basis for the induction of diabetes by streptozotocin. *Diabetes* 33: 771–777.
53. Chen, W., X. Liang, A. J. Peterson, D. H. Munn, and B. R. Blazar. 2008. The indoleamine 2,3-dioxygenase pathway is essential for human plasmacytoid dendritic cell-induced adaptive T regulatory cell generation. *J. Immunol.* 181: 5396–5404.
54. Andersson, A., M. Isaksson, J. Wefer, A. Norling, A. Flores-Morales, F. Rorsman, O. Kampe, R. A. Harris, and A. Lobell. 2008. Impaired autoimmune T helper 17 cell responses following DNA vaccination against rat experimental autoimmune encephalomyelitis. *PLoS One* 3: e3682.
55. Platten, M., P. P. Ho, S. Youssef, P. Fontoura, H. Garren, E. M. Hur, R. Gupta, L. Y. Lee, B. A. Kidd, W. H. Robinson, et al. 2005. Treatment of autoimmune neuroinflammation with a synthetic tryptophan metabolite. *Science* 310: 850–855.
56. Marta, M., A. Andersson, M. Isaksson, O. Kampe, and A. Lobell. 2008. Unexpected regulatory roles of TLR4 and TLR9 in experimental autoimmune encephalomyelitis. *Eur. J. Immunol.* 38: 565–575.
57. Kwidzinski, E., J. Bunse, O. Aktas, D. Richter, L. Mutlu, F. Zipp, R. Nitsch, and I. Bechmann. 2005. Indolamine 2,3-dioxygenase is expressed in the CNS and down-regulates autoimmune inflammation. *FASEB J.* 19: 1347–1349.
58. Wong, F. S., C. Hu, L. Zhang, W. Du, L. Alexopoulou, R. A. Flavell, and L. Wen. 2008. The role of Toll-like receptors 3 and 9 in the development of autoimmune diabetes in NOD mice. *Ann. NY Acad. Sci.* 1150: 146–148.
59. Koulmanda, M., A. Qipo, H. Auchincloss, Jr., and R. N. Smith. 2003. Effects of streptozotocin on autoimmune diabetes in NOD mice. *Clin. Exp. Immunol.* 134: 210–216.
60. Quintana, F. J., A. Rotem, P. Carmi, and I. R. Cohen. 2000. Vaccination with empty plasmid DNA or CpG oligonucleotide inhibits diabetes in nonobese diabetic mice: modulation of spontaneous 60-kDa heat shock protein autoimmunity. *J. Immunol.* 165: 6148–6155.
61. Von Herrath, M. 2009. Can we learn from viruses how to prevent type 1 diabetes? The role of viral infections in the pathogenesis of type 1 diabetes and the development of novel combination therapies. *Diabetes* 58: 2–11.

Corrections

Fallarino, F., C. Volpi, T. Zelante, C. Vacca, M. Calvitti, M. C. Fioretti, P. Puccetti, L. Romani, and U. Grohmann. 2009. IDO mediates TLR9-driven protection from experimental autoimmune diabetes. *J. Immunol.* 183: 6303–6312.

In Fig. 1*B*, the color key was incorrect. The results and conclusions of the article remain unchanged. The corrected Fig. 1*B* is shown below. The published legend for Fig. 1 is correct, but is shown again for reference.

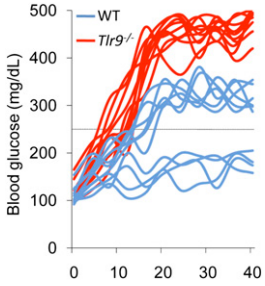

FIGURE 1. Higher susceptibility to STZ-induced diabetes in $Tlr9^{-/-}$ mice. WT ($n = 12$), $Tlr3^{-/-}$ ($n = 10$), and $Tlr9^{-/-}$ ($n = 10$) C57BL/6 mice were injected with STZ from day 1, and blood glucose was monitored over time (in *A–C*, one experiment is depicted of two with similar results). Diabetes was diagnosed in mice with blood glucose level >250 mg/dl. Mice were sacrificed at different times and analyzed for insulinemia (*D*) and pancreas histology (*E* and *F*) and immunohistochemistry (*E*). *A*, Average blood glucose in different groups is plotted over time. Data are presented as mean glucose levels ± SD. *, $p < 0.01$ ($Tlr9^{-/-}$ vs WT mice). *B*, Blood glucose concentrations over time in individual WT and $Tlr9^{-/-}$ mice. *C*, Incidence of diabetes over time in TLR-deficient and WT mice. $p < 0.01$ ($Tlr9^{-/-}$ vs WT mice). *D*, Blood insulin was measured by ELISA at day 30. Control, control animals treated with vehicle alone. Data are means ± SD of three experiments. *, $p < 0.05$ (STZ-treated $Tlr9^{-/-}$ vs WT mice). *E* and *F*, Pancreatic tissues were processed for H&E staining to evaluate insulitis (*E* and *F*) and immunostained for insulin (red, *E*). In fluorescent images, nuclei were counterstained with 4′,6-diamidino-2-phenylindole (blue). Representative islet area for each group (*E*) at day 40 and the percentages of islets per mouse with different score (*F*, see *Materials and Methods*) of lymphocyte infiltration (days 14 and 40) are shown. Percentages represented number of islets of a given score (see *Materials and Methods*) over total number of islets (30–40 per pancreas). *, $p < 0.01$ and **, $p < 0.001$ ($Tlr9^{-/-}$ vs WT mice).

www.jimmunol.org/cgi/doi/10.4049/jimmunol.1090041